On-Board Phase and Modulus Calibration of Large Aperture Synthesis Radiometers: Study Applied to MIRAS

F. Torres, A. Camps, J. Bará, I. Corbella, and R. Ferrero

Abstract—On-board calibration of bidimensional aperture synthesis radiometers with a large number of antennas by the standard correlated noise injection method is technologically very critical because of the stringent requirements on mass, volume, and phase equalization of the noise distribution network. A novel approach, which makes use of a set of uncorrelated noise sources uniformly distributed in the array, is proposed in this paper. Each noise source drives correlated noise only to a small set of adjacent antennas. These sets of antennas are overlapped in order to maintain phase and modulus track along the array. This approach reduces drastically mass and volume of the noise distribution network. Moreover, its phase matching requirement is strongly relaxed because it is only necessary within small sets of adjacent antennas. Power stability of the uncorrelated noise sources is also not a stringent requirement. This procedure allows independent phase and modulus calibration by making use of a reduced number of redundant correlations.

I. INTRODUCTION

A PERTURE synthesis radiometers are of increasing interest in on-board earth observation applications due to their reduced mass and volume requirements with relation to the traditional total power radiometers. Some works have already been performed to study fundamentals and practical limitations of these instruments [1], [2]. Recently, SMOS Conclusions and Recommendations [3] established the interest of such an instrument operating at 1.4 GHz in the measurement of soil moisture and ocean salinity, in order to develop hydrological cycle and climate models. SMOS has also conclude that, at present, "a single frequency, dual polarization instrument in a sun synchronous dawn-dusk orbit giving 0.5 K radiometric resolution, 10 km spatial resolution and 1–3 days revisit time would satisfy most user requirements" [3]. Within this scope, the European Space Agency (ESA) is currently carrying out the development of an L-band bidimensional interferometer radiometer called MIRAS (microwave imaging radiometer by aperture synthesis) [4]. The space-borne instrument is configured as a Y-shaped array with 43 antennas per arm spaced 0.89λ, plus the central one.

Phase and modulus calibration of the measured visibility samples is a major problem in a bidimensional synthesis array

radiometer. The correlated noise injection method has some advantages over methods based on phase and modulus closure relationships [6]. Noise injection allows calibration of the receiver parameters, independently of antenna imperfections such as coupling effects, pointing errors, etc. Once the receiver parameters are determined those antenna imperfections can be calibrated out of the measurement of a known scene, other external signal sources or by antenna ground testing. Moreover, correlated/uncorrelated noise injection allows calibration of errors that cannot be taken into account by phase and modulus relationships, such as receiver quadrature phase errors or voltage offsets at the digital correlators. On the other hand, noise injection implies increased hardware requirements and should be used only if errors not corrected by phase and modulus closure relationships have critical impact on system performance.

Correlated noise injection in arrays with a large number of antennas is technologically very critical because of the stringent requirements on mass, volume, and phase equalization of the noise distribution network. In this paper, we propose an approach that makes use of a set of uncorrelated noise sources uniformly distributed in the array. Each noise source drives correlated noise only to a small set of adjacent antennas. These sets of antennas are overlapped in order to maintain phase and modulus track along the array.

We start by modeling phase and amplitude receiver errors and writing the basic equations on which the calibration procedure is based. We continue by describing the calibration procedure, which is optimized in the sense of minimization of hardware requirements and number of measurements. The method is tested in order to verify the algorithms and to state the signal-to-noise ratio required to have a good estimation of the error coefficients. Finally, we derive some recommendations about how this calibration procedure should be implemented in a large bidimensional array, such as MIRAS.

This approach reduces drastically mass and volume of the noise distribution network in relation to the standard method, which uses a single correlated noise source [4], [5]. Moreover, phase matching requirement of the distribution network is strongly relaxed because it is only necessary within small sets of adjacent antennas. Power stability of the uncorrelated noise sources is also not a stringent requirement, because noise source temperatures are also estimated during calibration. As explained hereafter, this procedure allows independent phase and modulus calibration by making use of a reduced number of redundant correlations.
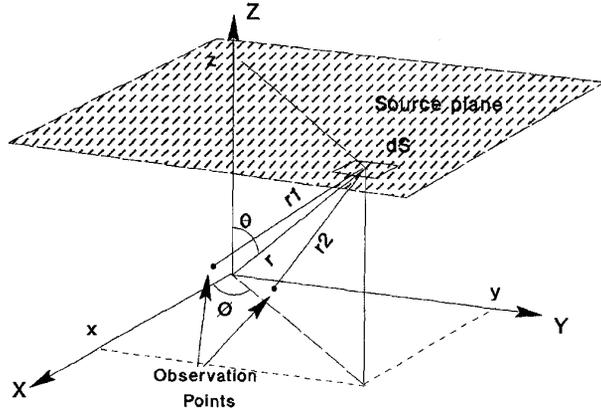
Fig. 1. Interferometer geometry. Antennas "1" and "2" are placed in the observation plane XY. Separation between both antennas in terms of λ sets a "baseline."

Fig. 2. Simplified block diagram of a single baseline MIRAS receiver.

II. BASIC EQUATIONS

While total power radiometers measure the power collected by a highly directive antenna, which directly gives the brightness temperature in the main beam direction, interferometer radiometers measure the correlation between pairs of nondirective antennas, giving samples of a function called "visibility" (baselines). For an ideal interferometer with equal receivers and antennas, the visibility function and the brightness temperature are related by a Fourier transform [1], [2]:

$$V(u, v) = K \iint_{\xi^2+\eta^2 \leq 1} T(\xi, \eta) e^{-j2\pi(u\xi+v\eta)} \, d\xi \, d\eta \quad (1)$$

$$T(\xi, \eta) = \frac{T_B(\xi, \eta)}{\sqrt{1 - \xi^2 - \eta^2}} \, |F_n(\xi, \eta)|^2 \quad (2)$$

where

1) (u, v) is the spacing between the two antennas in wavelengths;
2) $T_B(\xi, \eta)$ is the brightness temperature;
3) $T(\xi, \eta)$ (dimensions of K) will be called the modified brightness temperature;
4) $1/\sqrt{(1 - \xi^2 - \eta^2)}$ is the obliquity factor for a thermal source lying on a plane;
5) $F_n(\xi, \eta)$ is the normalized antenna voltage pattern;
6) $\xi = \sin\theta \cos\phi$, $\eta = \sin\theta \sin\phi$, the directing cosines (Fig. 1).

In Fig. 2, we have the simplified block diagram of MIRAS receiver relating the measurement of one baseline. The signals out of antennas "1" and "2," $s_1(t)$ and $s_2(t)$, are demodulated by a pair of coherent I/Q demodulators. The output of the receiver is the complex normalized visibility, given by

$$\mu = \mu_r + j\mu_j$$
$$= \frac{V_{12}(u, v)}{\sqrt{V_{11}(0, 0)V_{22}(0, 0)}}$$
$$= \frac{V_{12}(u, v)}{V(0, 0)} \quad (3)$$

$$V_{12}(u, v) = \frac{1}{2}E[S_{a1}(t)S_{a2}^*(t)] \quad (4)$$

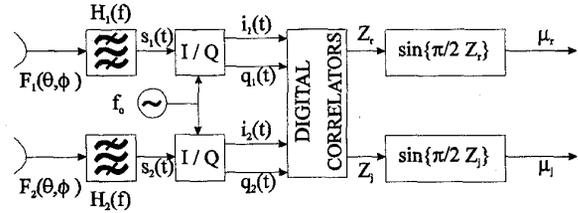where $V_{12}(u, v)$ is the visibility sample $V(u, v)$ measured between antennas "1" and "2," calculated as the cross-correlation of the analytical signals of $s_1(t)$ and $s_2(t)$, (4). $V(0, 0)$ is the scene averaged power kT_AB, assumed to be equal at the output of both antennas. As shown in Fig. 2, the real and imaginary parts of the normalized visibilities are computed by means of baseband real correlators as

$$\mu_r = \frac{\langle i_1(t)i_2(t)\rangle}{\sqrt{\langle i_1(t)i_1(t)\rangle \langle i_2(t)i_2(t)\rangle}}$$
$$= R_{i_1 i_2}(0) \quad (5)$$

$$\mu_j = \frac{\langle q_1(t)i_2(t)\rangle}{\sqrt{\langle q_1(t)q_1(t)\rangle \langle i_2(t)i_2(t)\rangle}}$$
$$= R_{q_1 i_2}(0) \quad (6)$$

where $i_1(t) = S_1(t) \cos\{\phi_1(t)\}$ and $q_1(t) = S_1(t) \sin\{\phi_1(t)\}$ are the in-phase and quadrature components of the narrow-band received signal at antenna "1" output $s_1(t) = S_1(t) \cos\{\omega t + [\phi_1(t)]\}$. MIRAS makes use of 1 bit-2 level digital correlators because of their low consumption, high speed and high degree of integration [4]. The outputs of the 1 bit-2 level digital correlators must be processed to derive the desired normalized visibilities μ_r and μ_j [7], as stated in Fig. 2.

III. MODELING AMPLITUDE AND PHASE ERRORS

Let the signal at the I/Q demodulator input of receiver "1" and "2" be

$$s_1^{raw}(t) = s_1(t) + n_1(t)$$
$$s_2^{raw}(t) = s_2(t) + n_2(t)$$

where $s_1(t)$ is the ideal signal and $n_1(t)$ zero mean narrow band Gaussian noise introduced by the receiver. If we take into account that $n_1(t)$ and $n_2(t)$ are uncorrelated signals of averaged power given by $kT_{R1}B$, and $kT_{R2}B$, being T_{R1} the receiver "1" noise temperature (see Appendix A for further insight). The measured normalized visibility can be written as

$$\mu_r^{raw} = \frac{\langle i_1^{raw}(t)i_2^{raw}(t)\rangle}{\sqrt{\langle i_1^{raw}(t)i_1^{raw}(t)\rangle \langle i_2^{raw}(t)i_2^{raw}(t)\rangle}}$$
$$= R_{i_1 i_2}^{raw}(0)$$
$$= g_1 g_2 \mu_r \quad (7)$$

$$\mu_j^{raw} = \frac{\langle q_1^{raw}(t)i_2^{raw}(t)\rangle}{\sqrt{\langle q_1^{raw}(t)q_1^{raw}(t)\rangle \langle i_2^{raw}(t)i_2^{raw}(t)\rangle}}$$
$$= R_{q_1 i_2}^{raw}(0)$$
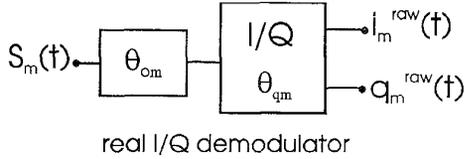$$= g_1 g_2 \mu_j \quad (8)$$

real I/Q demodulator

Fig. 3. I/Q receiver model including in-phase and quadrature errors θ_{om} and θ_{qm}.

where

$$g_1 = \left(1 + \frac{T_{R1}}{T_A}\right)^{-(1/2)}$$

$$g_2 = \left(1 + \frac{T_{R2}}{T_A}\right)^{-(1/2)}. \qquad (9)$$

If phase errors are taken into account, the I/Q demodulator can be modeled as in Fig. 3. In this case, the in-phase and quadrature components of the measured signal in receiver "1" can be written as

$$s_1(t) = S_1(t) \cos[\omega t + \phi_1(t)]$$

$$i_1^{\mathrm{raw}}(t) = S_1(t) \cos\left[\phi_1(t) + \theta_{o1} + \frac{\theta_{q1}}{2}\right]$$

$$q_1^{\mathrm{raw}}(t) = S_1(t) \sin\left[\phi_1(t) + \theta_{o1} - \frac{\theta_{q1}}{2}\right] \qquad (10)$$

in which θ_{o1} is the receiver in-phase error, and θ_{q1} its quadrature error. Note that θ_{q1}, has been split into the I and Q demodulator outputs. It has been done so to simplify calibration procedures. Now, if both amplitude and phase errors are considered, let us simplify notation by defining

$$\mu_{ii} = \overline{R_{i_1 i_2}^{\mathrm{raw}}(0)}$$

$$\mu_{qi} = \overline{R_{q_1 i_2}^{\mathrm{raw}}(0)} \qquad (11)$$

and the measured normalized visibilities can be expressed as (12), shown at the bottom of the page. Note, that the measured normalized visibility can also be computed in an alternative way. Saying

$$\mu_{qq} = \overline{R_{q_1 q_2}^{\mathrm{raw}}(0)}$$

$$\mu_{iq} = \overline{R_{i_1 q_2}^{\mathrm{raw}}(0)} \qquad (13)$$

the measured visibility can also be written as (14), shown at the bottom of the page.

The alternative measurements of μ_r^{raw} and μ_j^{raw} do not require that the number of correlators devoted to calibration is doubled. During calibration the I/Q signals of each receiver

can be interchanged at the input of the correlation distribution matrix. In this way, the system first measures μ_{ii} and μ_{qi} and, after switching I/Q channels, it measures μ_{qq} and μ_{iq}.

To summarize, we have a matrix P_k that allows us to simulate each measured visibility out of the ideal visibility when phase and amplitude receiver errors are present. k is the number of measured visibilities, redundant or not. It is

$$\mu^{\mathrm{raw}} = P_k \mu. \qquad (15)$$

Note that P_k is a 2×2 matrix which depends on the antenna pair "mn" used to measure such visibility, and also depends on how μ^{raw} is computed.

IV. CALIBRATION BY CORRELATED NOISE INJECTION

If zero-mean, narrow band Gaussian correlated noise is injected at receiver "m" and "n" inputs, the ideal normalized visibility is the normalized auto-correlation of the noise signal evaluated at $\tau = 0$, which gives $\mu_r = 1$, $\mu_j = 0$. The unknowns θ_{om}, θ_{on}, θ_{qm}, θ_{qn}, T_{Rm}, and T_{Rn} can be derived out of the measured visibilities μ_r^{raw} and μ_j^{raw}. However, it must be guaranteed that correlated noise is correctly distributed to all antennas. The standard method makes use of a single noise source [4], [5], but in a large array it is very difficult to maintain phase equalization of the noise distribution network through the operating temperature range. Moreover, in MIRAS, correlated noise must be distributed to 130 antennas, which gives the noise distribution network impossible mass and volume requirements if signal paths delays are to be equalized. We propose the following solution which reduces drastically hardware requirements of the distribution network.

A. A Correlated Noise Distribution Network

Fig. 4 shows the noise distribution network that is proposed in this paper. It makes use of 31 uncorrelated sources each one driving correlated noise to a set of eight antennas. As it is shown, each antenna receives noise from two adjacent sources. This allows phase and amplitude calibration of the array. The source n_0 delivers power to the 10 central antennas in order to keep good phase and modulus track between the three arms of MIRAS Y-shaped array. This noise source must be monitored with good accuracy so as to perform amplitude calibration of the whole set of visibility samples.

Fig. 5 gives a detail of noise distribution along a single arm. Antennas $a_0 \cdots a_7$ receive correlated noise only from source n_1, therefore the largest baseline we can compute is 7 times the basic baseline. As shown in Fig. 5, we used 14 correlations within each set of eight antennas in order to solve in-phase,

$$\begin{pmatrix} \mu_{ii} \\ \mu_{qi} \end{pmatrix} = g_1 g_2 \begin{bmatrix} \cos\left(\theta_{o2} - \theta_{o1} + \frac{\theta_{q2}}{2} - \frac{\theta_{q1}}{2}\right) & \sin\left(\theta_{o2} - \theta_{o1} + \frac{\theta_{q2}}{2} - \frac{\theta_{q1}}{2}\right) \\ -\sin\left(\theta_{o2} - \theta_{o1} + \frac{\theta_{q2}}{2} + \frac{\theta_{q1}}{2}\right) & \cos\left(\theta_{o2} - \theta_{o1} + \frac{\theta_{q2}}{2} + \frac{\theta_{q1}}{2}\right) \end{bmatrix} \begin{pmatrix} \mu_r \\ \mu_j \end{pmatrix} \qquad (12)$$

$$\begin{pmatrix} \mu_{qq} \\ \mu_{iq} \end{pmatrix} = g_1 g_2 \begin{bmatrix} \cos\left(\theta_{o2} - \theta_{o1} - \frac{\theta_{q2}}{2} + \frac{\theta_{q1}}{2}\right) & \sin\left(\theta_{o2} - \theta_{o1} - \frac{\theta_{q2}}{2} + \frac{\theta_{q1}}{2}\right) \\ \sin\left(\theta_{o2} - \theta_{o1} - \frac{\theta_{q2}}{2} - \frac{\theta_{q1}}{2}\right) & -\cos\left(\theta_{o2} - \theta_{o1} - \frac{\theta_{q2}}{2} - \frac{\theta_{q1}}{2}\right) \end{bmatrix} \begin{pmatrix} \mu_r \\ \mu_j \end{pmatrix} \qquad (14)$$
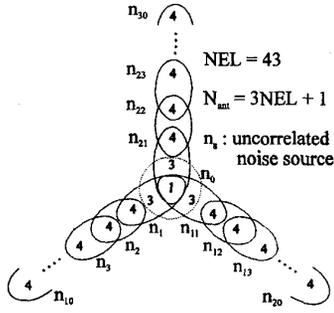
Fig. 4. Proposed noise distribution network. It makes use of 31 distributed uncorrelated noise sources, each one driving power to a set of eight adjacent antennas. These sets of antennas are overlapped to allow phase and modulus calibration of the array.
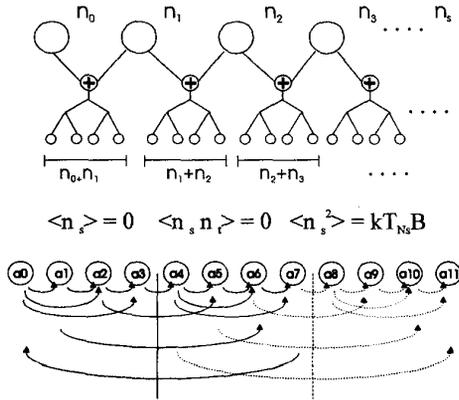

Fig. 5. Detail of noise distribution along an arm. Correlations that are performed within each set of eight antennas. This configuration minimizes the number of correlations.

quadrature and modulus errors of these sets of antennas. Now if we shift 4 antennas away from a_0, we have a new set of eight antennas to repeat the procedure. Antennas $a_4 \cdots a_7$ are common to the previous set allowing phase and modulus track along the arm. As will be shown later, errors do not increase significantly along the arms when performing this calibration procedure.

Since antennas are separated 0.89λ [4], each arm requires 63 coaxial cables of about 50 cm to distribute correlated noise from 10 noise sources (Figs. 3 and 4). If we account 40 gr/m, this makes 1.26 Kg, uniformly distributed along each arm. In the other hand, a single noise source placed at the center of the array, requires 43 coaxial cables 8.3 m long each to keep path delay equalization (the arm length). This makes 14.3 Kg/arm, not uniformly distributed. Moreover, such long cables will have unmatched phase drifts due to thermal gradients across the instrument.

In conclusion, the main advantage of this approach is that it reduces drastically mass and volume of the noise distribution network since only short length matched coaxial lines are required. Moreover, its phase matching requirement is strongly relaxed because it is only necessary within sets of eight adjacent antennas. Only unbalanced phase drift due to temperature variations must be minimized. The calibration procedure determines noise source temperatures out of the knowledge of n_0, and, hence, simple nonstabilized diodes can

be used as noise sources. As shown hereafter, it is possible to calibrate phase and amplitude independently with reduced hardware requirements.

B. Phase Calibration

Note that, once the correlated noise is injected, $\mu_j = 0$, and the gain factor $g_m g_n$ can be eliminated by dividing the measured real and imaginary parts of the visibilities. If we take into account the two alternative procedures to derive the measured normalized visibility, we have a set of two equations out of each pair of antennas:

$$-\mu_{ii} \sin\left(\theta_{on} - \theta_{om} + \frac{\theta_{qn}}{2} + \frac{\theta_{qm}}{2}\right)$$

$$= \mu_{qi} \cos\left(\theta_{on} - \theta_{om} + \frac{\theta_{qn}}{2} - \frac{\theta_{qm}}{2}\right)$$

$$\mu_{qq} \sin\left(\theta_{on} - \theta_{om} - \frac{\theta_{qn}}{2} - \frac{\theta_{qm}}{2}\right)$$

$$= \mu_{iq} \cos\left(\theta_{on} - \theta_{om} - \frac{\theta_{qn}}{2} + \frac{\theta_{qm}}{2}\right). \tag{16}$$

As shown in Fig. 5 correlated noise is driven simultaneously to a set of eight adjacent antennas. If we consider one of these sets of eight antennas, we have 16 unknowns ($8\theta_o$, and $8\theta_q$) to be derived out of 28 equations (14 pairs of antennas). The system must be overdetermined in order to keep good phase track along the arms when overlapping sets of eight antennas. Overdetermination is also required to prevent that failure of any antenna or correlator makes the whole calibration unfeasible.

C. Modulus Calibration

Once the phase terms are known, the gain factors $g_m g_n$ can be estimated. Unfortunately these gain factors are not those which are required. During calibration the antenna temperatures T_{Am} and T_{An} are in fact the correlated noise source temperatures. Therefore, it is necessary to estimate the receiver noise temperatures T_{Rm} and T_{Rn} before computing the gain factors out of the scene average temperature T_A given by the total power. At this point one must note that, in order to estimate the receiver noise temperatures, it is necessary that only one noise source is driving each set of eight antennas that are simultaneously under calibration. Hence, calibration is performed by measuring visibilities, first with the even noise sources ON and the odd sources OFF, and, afterwards, with the even noise sources OFF and the odd sources ON. From Fig. 5 we see that if we proceed in this way, we have sets of eight antennas driven by a single noise source. Since contiguous sets of eight antennas are overlapped, phase and modulus track is maintained along the array arms.

Now, if we take into account the first set of four antennas $(a_0 \cdots a_3)$ in Fig. 5, which are driven by the even noise source T_{N0} (T_{N1} OFF), we get the even coefficient

$$K_{mn}^0 = \frac{1}{g_m^2 g_n^2} = \left(1 + \frac{T_{Rm}}{T_{N0}}\right)\left(1 + \frac{T_{Rn}}{T_{N0}}\right) \tag{17}$$

out of the correlations performed between antennas "m" and "n." T_{Rm} and T_{Rn} are the receiver "m" and "n" noise

temperatures. Note that, once the phase coefficients are already determined, K_{mn}^0 can be averaged out of four values. In order to linearize the system of equations we can take logarithms

$$\log K_{mn}^0 = \log\left(1 + \frac{T_{Rm}}{T_{N0}}\right) + \log\left(1 + \frac{T_{Rn}}{T_{N0}}\right)$$

$$a_{mn}^0 = x_{om} + x_{on} \qquad (18)$$

where x_{om} stands for a linear coefficient related to antenna "m" when driven by the noise source T_{N0}. If we look at the correlations which relate antennas within the first set of four elements $(a_0 \cdots a_3)$, we can derive the linear system

$$\begin{pmatrix} 1 & 1 & 0 & 0 \\ 0 & 1 & 1 & 0 \\ 0 & 0 & 1 & 1 \\ 1 & 0 & 1 & 0 \\ 1 & 0 & 0 & 1 \end{pmatrix} \begin{pmatrix} x_{o0} \\ x_{o1} \\ x_{o2} \\ x_{o3} \end{pmatrix} = \begin{pmatrix} a_{01}^0 \\ a_{12}^0 \\ a_{23}^0 \\ a_{02}^0 \\ a_{03}^0 \end{pmatrix}. \qquad (19)$$

This is $Ax_0 = a^0$. The linear coefficients are determined as $x_0 = A^{-1}a^0$, where A^{-1} is the pseudo-inverse of A. Now, providing that T_{N0} is known, the receiver noise temperatures are directly

$$T_{Rm} = T_{N0}(10^{x_{om}} - 1). \qquad (20)$$

Once the receiver temperatures of $a_0 \cdots a_3$ are determined, we can proceed by switching OFF the even noise source T_{N0}. and switching ON the unknown odd noise source T_{N1}. T_{N1} can be estimated easily out of the average

$$T_{N1} = \langle T_{Rm}(10^{x_{1m}} - 1)^{-1}\rangle. \qquad (21)$$

Now x_{1m} is the linear coefficient of antenna "m" when driven by the odd noise source T_{N1}. Once T_{N1} is determined we can repeat this procedure with the second set of antennas $a_4 \cdots a_7$ and the unknown even noise source T_{N2}. This iterative procedure ends with all the receiver noise temperatures T_{Rm} and noise source temperatures T_{Ns} determined.

The above procedure is based on the knowledge of T_{N0}. Hence, the accuracy of modulus calibration is highly dependent on the accuracy of T_{N0}. In this approach, T_{N0} is placed at the center of the array (Fig. 4) to allow modulus calibration of the three arms. T_{N0} can be determined either by switching during calibration the total power to measure this noise source, or by dedicating a special power measurement unit.

D. Calibration Implementation

Obviously, calibration procedures must be optimized in order to minimize hardware requirements and number of measurements. In this sense, the calibration method just described can be implemented as follows.

a) Switch EVEN noise sources ON and ODD noise sources OFF. Set the correlation distribution matrix to measure μ_{ii} and μ_{qi}. Measure correlations within each set of eight antennas which is driven by the same EVEN noise source. Average measurements in order to increase signal-to-noise ratio.

b) Set the correlation distribution matrix to measure μ_{qq} and μ_{iq}. Measure correlations within each set of eight antennas which is driven by the same EVEN noise

source. Average measurements in order to increase signal-to-noise ratio.

c) Switch EVEN noise sources OFF and ODD noise sources ON. Set the correlation distribution matrix to measure μ_{ii} and μ_{qi}. Measure correlations within each set of eight antennas which is driven by the same ODD noise source. Average measurements in order to increase signal-to-noise ratio.

d) Set the correlation distribution matrix to measure μ_{qq} and μ_{iq}. Measure correlations within each set of eight antennas which is driven by the same ODD noise source. Average measurements in order to increase signal-to-noise ratio.

e) Set in-phase error of the antenna 0 (at the center of the array) to $\theta_{o0} = 0$. Solve the set of equations that relate antenna phases by a minimization method.

f) Measure the noise source temperature T_{N0} and apply the iterative method to determine the receiver noise temperatures. Measure the scene average power T_A to compute each receiver gain factors as

$$g_m = \left(1 + \frac{T_{Rm}}{T_A}\right)^{-(1/2)}. \qquad (22)$$

g) Compute the calibration matrices P_k^{-1} out of the error coefficients of each antenna. Note that P_k^{-1} must be computed for all the visibilities that are measured during scene exploration.

$$\mu = P_k^{-1} \mu^{\text{raw}}. \qquad (23)$$

V. TESTING THE METHOD

To test the proposed calibration procedure we require a set of measured visibilities corrupted by receiver phase and modulus errors. If we want to take into account the finite integration time of the correlators those visibilities must also be corrupted by additive noise. We first proceed by defining the error coefficients of a real receiver and generating the measured visibilities, corrupted by noise. After calibration, this will allow comparison between real and recovered receiver error coefficients.

A. Simulating the Measured Normalized Visibilities

A real instrument is modeled out of a matrix C of error coefficients, defined as

$$\overline{\overline{C}} = \begin{pmatrix} 0 & \theta_{q0} & T_{R0} & T_{N0} \\ \theta_{o1} & \theta_{q1} & T_{R1} & \vdots \\ \vdots & \vdots & \vdots & T_{Ns} \\ \vdots & \vdots & \vdots & 0 \\ \theta_{op} & \theta_{qp} & T_{Rp} & \vdots \end{pmatrix} \qquad (24)$$

where p is the number of antennas in the array and s the number of noise sources. Note that the central antenna sets the phase reference, it is $\theta_{o0} = 0$. The phases of the receivers have a zero mean Gaussian distribution with standard deviation $\sigma_{\theta o}$ and $\sigma_{\theta q}$. The noise temperatures have also a Gaussian distribution of means $T_R = 80$ K and $T_N = 300$ K, and standard deviations σ_{TR} and σ_{TN}. For calibration purposes,

T_{N0} is considered to be known with enough accuracy. Once the receiver coefficients are generated we proceed to compute the matrix $P(C)$ that simulates the real receiver as

$$P(\overline{\overline{C}}) = \begin{pmatrix} P_1 & 0 & \cdots & 0 \\ 0 & P_2 & \cdots & 0 \\ \vdots & \vdots & \ddots & \vdots \\ 0 & 0 & \cdots & P_k \end{pmatrix}. \qquad (25)$$

$P(C)$ is a sparse matrix, whose diagonal is composed by 2×2 matrices P_k that relate the ideal normalized visibilities with their measured counterparts. k is the number of visibility samples, redundant or not, that are measured during calibration. Note that we have to compute four $P(C)$ matrices to account for the following measurements:

1) Even T_{Ns} ON, odd T_{Ns} OFF.

   Measure of μ_{ii} and μ_{qi}

2) Even T_{Ns} ON, odd T_{Ns} OFF.

   Measure of μ_{qq} and μ_{iq}

3) Even T_{Ns} OFF, odd T_{Ns} ON.

   Measure of μ_{ii} and μ_{qi}

4) Even T_{Ns} OFF, odd T_{Ns} ON.

   Measure of μ_{qq} and μ_{iq}.

Now we can compute the measured visibilities from matrices $P(C)$ as

$$\begin{pmatrix} \mu_{r_1} \\ \mu_{j_1} \\ \vdots \\ \mu_{r_k} \\ \mu_{j_k} \end{pmatrix}^{raw} = P(\overline{\overline{C}}) \begin{pmatrix} \mu_{r_1} + n_{r_1} \\ \mu_{j_1} + n_{j_1} \\ \vdots \\ \mu_{r_k} + n_{r_k} \\ \mu_{j_k} + n_{j_k} \end{pmatrix}. \qquad (26)$$

The ideal visibilities μ_k when measuring correlated noise are $\mu_{rk} = 1$ and $\mu_{jk} = 0$. However, we added zero mean Gaussian noise $n_k = n_{rk} + jn_{jk}$ to account for the correlators finite integration time (0.3 s) [4]. The noise is specified out of the signal to noise ratio—which is equivalent to specify different integration times

$$\left(\frac{S}{N}\right) = \frac{1}{\sigma_v} = \frac{1}{\sqrt{2 < n_{rk}^2 >}} = \frac{1}{\sqrt{2 < n_{jk}^2 >}} \qquad (27)$$

where σ_v is the standard deviation of the visibilities. σ_v in MIRAS it is about 36 dB due to the finite integration time (0.3 s). However, during calibration integration time is not limited—antenna movement do not affect noise injection—and the signal-to-noise ratio can be increased by averaging measurements. It is, averaging 100 measurements (30 s integration time) gives and increase in signal-to-noise ratio of 10 dB, which will suffice.

B. Simulation Results

In order to validate the method, we modeled MIRAS receiver errors as $\sigma_{\theta o} = 15°$, $\sigma_{\theta q} = 5°$, $T_R = 80$ K, $\sigma_{TR} = 15$ K, $T_N = 300$ K, and $\sigma_{TN} = 30$ K [4]. Then, we simulated a set of measured normalized visibilities μ^{raw} and recovered the coefficients using the calibration procedure

TABLE I
PHASE AND MODULUS RESIDUAL CALIBRATION ERRORS

S/N	σ_{0o}	σ_{0q}	$\sigma_{\Delta TR}$
35 dB	0.0198°	0.0138°	1.3 K
40 dB	0.0031°	0.0039°	0.2 K
45 dB	0.0007°	0.0017°	0.07 K

explained in the previous paragraphs. The estimated coefficient errors are summarized in Table I. In the plots of Fig. 6, we see the absolute error in each antenna, which do not increase significantly along the arms. Note that, when measurements are only corrupted by Gaussian noise, errors on estimated phases are negligible. In the other hand, errors in the receiver noise temperature estimation are somewhat significant and some averaging could be required depending on the radiometric sensitivity that is required.

In order to set MIRAS snap-shot radiometric resolution below $\Delta T \leq 0.4$ K (over a constant scene of 300 K), phase errors must be estimated with $\sigma_\phi \leq 0.5°$ and amplitude errors with $\sigma_{\Delta\mu} \leq 10^{-3}$ [8]. Therefore, calibrated receiver phase errors contribution to radiometric resolution is negligible. In Appendix B, it is shown that an amplitude error of $\sigma_{\Delta\mu} \leq 10^{-3}$ requires that the receiver noise temperatures are recovered with $\sigma_{\Delta TR} \leq 0.5$ K. The reference noise source temperature T_{N0} can be measured with enough accuracy with a total power radiometer, and a signal-to-noise ratio of at least 40 dB must be achieved to recover receiver noise temperatures [Fig. 5(c)].

VI. HARDWARE REQUIREMENTS

As explained before, this method uses as reference the phase of the central antenna, which is set to $\theta_{oo} = 0$. This do not introduce any error since a phase offset equal in all the antennas do not affect visibilities. The reference temperature T_{N0} must be measured with a resolution of about 0.5 K, if MIRAS radiometric resolution is not to be degraded [8]. Integration time must be increased at least to gives S/N of 40 dB. However, this method imposes other requirements if calibration is to succeed:

- This calibration procedure estimates phase and temperature errors relating each receiver. Visibility phase and gain errors are computed out of this estimation. Hence, non separable terms caused by, for instance, filter misalignments, must be minimized. These are not calibrated terms and remain as residual errors.
- Voltage offset errors must be removed from the measured visibilities prior to phase and modulus calibration. Uncorrelated noise injection or ground testing—plus offset drift minimization—should be used.
- During calibration, the correlated noise is injected at the antenna outputs. Therefore, antenna contribution to the receiver noise temperature is not measured and must be taken into account when computing de calibration matrices P_k^{-1}. This is, the receiver noise when exploring a scene is the estimated receiver noise temperature plus the antenna noise contribution This is given by $T_{Ram} = T_{phi}(1 - \eta_{am})$, where T_{phi} is the physical temperature
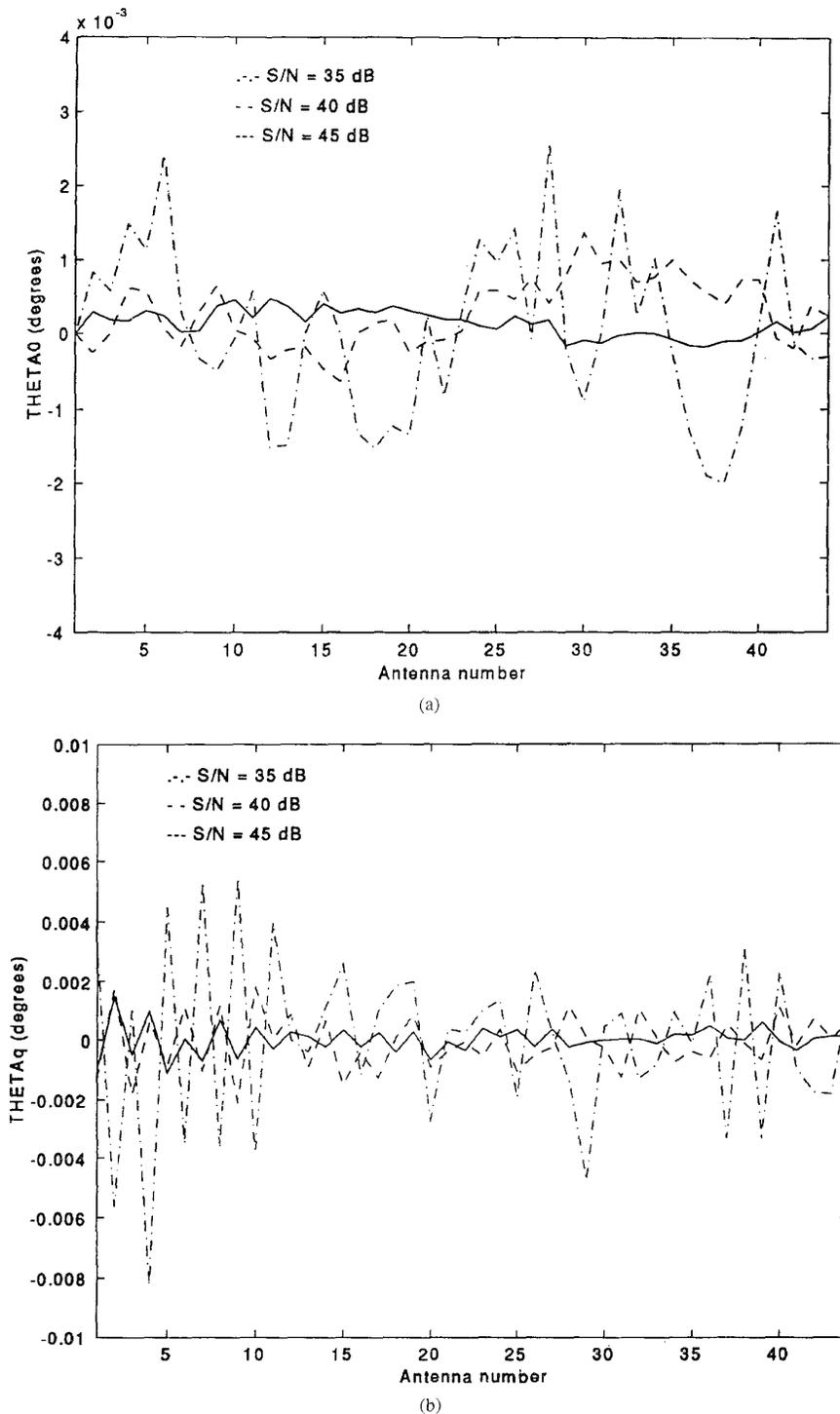
(a)

(b)

Fig. 6.   Absolute calibration residual errors along the arm. S/N - · -- 35 dB. - - - 40 dB. ―――― 45 dB. (a) Absolute in-phase residual error $\Delta\theta_{om}$ along the arm. (b) Absolute quadrature residual error $\Delta\theta_{qm}$ along the arm.

of the antenna and η_{am} the antenna loss. If $\eta_{am} = 0.5$ dB and ΔT_{Ri} is constrained to 0.5 K, then the physical temperature of the antenna must be monitored within 5 K and η_{am} measured within 0.1%.

• It is straight forward to demonstrate that the estimated receiver in-phase error includes the phase unbalance of the correlated noise power distribution network. In order to remove this contribution from the estimated in-phase error, the distribution network must be ground calibrated and unbalanced phase drifts due to temperature constrained to $\sigma_\phi \le 0.5°$ [8]. These in-phase errors do not affect quadrature and amplitude error estimation.
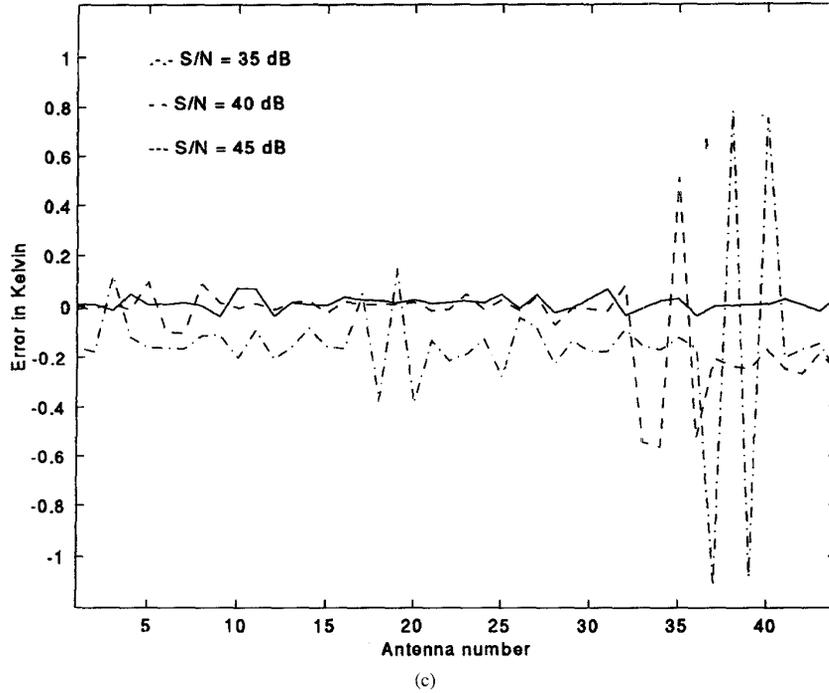
Fig. 6. *(Continued.)* (c) Absolute receiver temperature residual error ΔT_{Rm} along the arm.

VII. CONCLUSION

In this paper, a new phase and modulus calibration approach, based on the correlated noise injection method has been proposed. This method makes use of a set of uncorrelated noise sources uniformly distributed in the array, each one driving correlated noise to a small set of adjacent antennas. These sets of antennas are overlapped in order to keep phase and modulus track along the arms of the array.

Basic equations and procedures on which the calibration procedure is based have been presented. Simulations have validated the method to calibrate a large aperture synthesis radiometer such as MIRAS, thus providing a drastic mass and volume reduction of the noise distribution network, with minimum hardware requirements.

APPENDIX A

In this appendix, we derive the relationship between the ideal visibility samples and the measured visibilities when both in-phase and quadrature errors are present.

Let have a real zero-mean narrow-band Gaussian signal centered at ω_o

$$s_1(t) = S_1(t) \cos\{\omega_o t + \phi_1(t)\}. \tag{A-1}$$

The output of a coherent I/Q demodulator is given by

$$i_1(t) = S_1(t) \cos \phi_1(t)$$
$$q_1(t) = S_1(t) \sin \phi_1(t). \tag{A-2}$$

However, if an in-phase error θ_{o1} and a quadrature error θ_{q1} is introduced by the receiver, then we can write for the measured

in-phase and quadrature baseband signals

$$i_1^{\text{raw}}(t) = S_1(t) \cos\left(\phi_1(t) + \theta_{o1} + \frac{\theta_{q1}}{2}\right)$$
$$q_1^{\text{raw}}(t) = S_1(t) \sin\left(\phi_1(t) + \theta_{o1} - \frac{\theta_{q1}}{2}\right). \tag{A-3}$$

Note that, for calibration purposes, the quadrature error has been split into two terms. The visibility sample related to antennas "1" and "2" is calculated in MIRAS by means of baseband real correlators [4] as

$$V_{12}(u, v) = R_{i_1 i_2}(0) + j R_{q_1 i_2}(0). \tag{A-4}$$

Hence, in the ideal case, the real and imaginary parts of the visibility function are

$$V_r(u, v) = R_{i_1 i_2}(0)$$
$$= \langle S_1 \cos(\phi_1) S_2 \cos(\phi_2) \rangle$$
$$= \langle S_1 S_2 \rangle \langle \cos(\phi_1) \cos(\phi_2) \rangle$$
$$V_j(u, v) = R_{q_1 i_2}(0)$$
$$= \langle S_1 \sin(\phi_1) S_2 \cos(\phi_2) \rangle$$
$$= \langle S_1 S_2 \rangle \langle \sin(\phi_1) \cos(\phi_2) \rangle \tag{A-5}$$

where, for the sake of simplicity, time dependence of the magnitudes has been omitted. In the other hand, if phase errors are taken into account, the measured visibility can now be written as

$$V_{12}^{\text{raw}}(u, v) = R_{i_1 i_2}^{\text{raw}}(0) + j R_{q_1 i_2}^{\text{raw}}(0) \tag{A-6}$$

where

$$V_r^{\text{raw}}(u, v) = R_{i_1 i_2}^{\text{raw}}(0)$$

$$= \left\langle S_1 \cos\left(\phi_1 + \theta_{01} + \frac{\theta_{q1}}{2}\right) \right.$$
$$\left. \cdot S_2 \cos\left(\phi_2 + \theta_{02} + \frac{\theta_{q2}}{2}\right) \right\rangle$$

$$= \langle S_1 S_2 \rangle \left\langle \cos\left(\phi_1 + \theta_{01} + \frac{\theta_{q1}}{2}\right) \right.$$
$$\left. \cdot \cos\left(\phi_2 + \theta_{02} + \frac{\theta_{q2}}{2}\right) \right\rangle$$

$$= \langle S_1 S_2 \rangle \left\langle \left[\cos\phi_1 \cos\left(\theta_{01} + \frac{\theta_{q1}}{2}\right) \right.\right.$$
$$\left. - \sin\phi_1 \sin\left(\theta_{01} + \frac{\theta_{q1}}{2}\right) \right]$$
$$\cdot \left[\cos\phi_2 \cos\left(\theta_{02} + \frac{\theta_{q2}}{2}\right) \right.$$
$$\left.\left. - \sin\phi_2 \sin\left(\theta_{02} + \frac{\theta_{q2}}{2}\right) \right] \right\rangle. \quad \text{(A-7)}$$

The parenthesis can be expanded to yield

$$R_{i_1 i_2}^{\text{raw}}(0) =$$
$$\langle S_1 S_2 \rangle \left\{ \langle \cos\phi_1 \cos\phi_2 \rangle \right.$$
$$\cdot \cos\left(\theta_{01} + \frac{\theta_{q1}}{2}\right) \cos\left(\theta_{02} + \frac{\theta_{q2}}{2}\right)$$
$$- \langle \cos\phi_1 \sin\phi_2 \rangle \cos\left(\theta_{01} + \frac{\theta_{q1}}{2}\right) \sin\left(\theta_{02} + \frac{\theta_{q2}}{2}\right)$$
$$- \langle \sin\phi_1 \cos\phi_2 \rangle \sin\left(\theta_{01} + \frac{\theta_{q1}}{2}\right) \cos\left(\theta_{02} + \frac{\theta_{q2}}{2}\right)$$
$$\left. + \langle \sin\phi_1 \sin\phi_2 \rangle \sin\left(\theta_{01} + \frac{\theta_{q1}}{2}\right) \sin\left(\theta_{02} + \frac{\theta_{q2}}{2}\right) \right\}.$$
$$\text{(A-8)}$$

Writing last equation as a function of the ideal correlations

$$R_{i_1 i_2}^{\text{raw}}(0) =$$
$$\left\{ R_{i_1 i_2}(0) \cos\left(\theta_{01} + \frac{\theta_{q1}}{2}\right) \cos\left(\theta_{02} + \frac{\theta_{q2}}{2}\right) \right.$$
$$- R_{i_1 q_2}(0) \cos\left(\theta_{01} + \frac{\theta_{q1}}{2}\right) \sin\left(\theta_{02} + \frac{\theta_{q2}}{2}\right)$$
$$- R_{q_1 i_2}(0) \sin\left(\theta_{01} + \frac{\theta_{q1}}{2}\right) \cos\left(\theta_{02} + \frac{\theta_{q2}}{2}\right)$$
$$\left. + R_{q_1 q_2}(0) \sin\left(\theta_{01} + \frac{\theta_{q1}}{2}\right) \sin\left(\theta_{02} + \frac{\theta_{q2}}{2}\right) \right\}. \quad \text{(A-9)}$$

Taking into account that, for narrow-band symmetric Gaussian signal

$$R_{i_1 i_2}(0) = R_{q_1 q_2}(0)$$
$$R_{q_1 i_2}(0) = -R_{i_1 q_2}(0). \quad \text{(A-10)}$$

Then

$$R_{i_1 i_2}^{\text{raw}}(0) = R_{i_1 i_2}(0) \cos\left(-\theta_{01} - \frac{\theta_{q1}}{2} + \theta_{02} + \frac{\theta_{q2}}{2}\right)$$
$$- R_{q_1 i_2}(0) \sin\left(-\theta_{01} + \frac{\theta_{q1}}{2} - \theta_{02} - \frac{\theta_{q2}}{2}\right)$$

$$= V_r \cos\left(\theta_{02} - \theta_{01} + \frac{\theta_{q2}}{2} - \frac{\theta_{q1}}{2}\right)$$
$$+ V_j \sin\left(\theta_{02} - \theta_{01} + \frac{\theta_{q2}}{2} - \frac{\theta_{q1}}{2}\right). \quad \text{(A-11)}$$

We can proceed in a similar way to calculate the measured imaginary part of the visibility

$$V_j^{\text{raw}}(u, v) = R_{q_1 i_2}^{\text{raw}}(0)$$
$$= \left\langle S_1 \sin\left(\phi_1 + \theta_{01} - \frac{\theta_{q1}}{2}\right) \right.$$
$$\left. \cdot S_2 \cos\left(\phi_2 + \theta_{02} + \frac{\theta_{q2}}{2}\right) \right\rangle$$
$$= \langle S_1 S_2 \rangle \left\langle \sin\left(\phi_1 + \theta_{01} - \frac{\theta_{q1}}{2}\right) \right.$$
$$\left. \cdot \cos\left(\phi_2 + \theta_{02} + \frac{\theta_{q2}}{2}\right) \right\rangle$$
$$= \langle S_1 S_2 \rangle \left\langle \left[\sin\phi_1 \cos\left(\theta_{01} - \frac{\theta_{q1}}{2}\right) \right.\right.$$
$$\left. + \cos\phi_1 \sin\left(\theta_{01} - \frac{\theta_{q1}}{2}\right) \right]$$
$$\cdot \left[\cos\phi_2 \cos\left(\theta_{02} + \frac{\theta_{q2}}{2}\right) \right.$$
$$\left.\left. - \sin\phi_2 \sin\left(\theta_{02} + \frac{\theta_{q2}}{2}\right) \right] \right\rangle. \quad \text{(A-12)}$$

Arranging terms as done before results in

$$R_{q_1 i_2}^{\text{raw}}(0) = R_{q_1 i_2}(0) \sin\left(\theta_{01} - \frac{\theta_{q1}}{2} - \theta_{02} - \frac{\theta_{q2}}{2}\right)$$
$$+ R_{q_1 i_2}(0) \cos\left(\theta_{01} - \frac{\theta_{q1}}{2} - \theta_{02} - \frac{\theta_{q2}}{2}\right)$$
$$= -V_r \sin\left(\theta_{02} - \theta_{01} + \frac{\theta_{q2}}{2} + \frac{\theta_{q1}}{2}\right)$$
$$+ V_j \cos\left(\theta_{02} - \theta_{01} + \frac{\theta_{q2}}{2} + \frac{\theta_{q1}}{2}\right). \quad \text{(A-13)}$$

Finally, the relationship between the ideal and the measured visibility sample can be expressed as (A-14), shown at the top of the next page. We can calculate

$$R_{i_1 i_2}^{\text{raw}}(0) \neq R_{q_1 q_2}^{\text{raw}}(0)$$
$$R_{q_1 i_2}^{\text{raw}}(0) \neq -R_{i_1 q_2}^{\text{raw}}(0). \quad \text{(A-15)}$$

Proceeding in as before it is straightforward to arrive at (A-16), shown at the top of the next page. Note that in each row of these matrices the phases are arranged in linearly independent equations. This can be used to increase the number of equations when calibrating the phases.

APPENDIX B

This appendix is devoted to the derivation of the relationship between the error in the receiver noise temperature estimation and visibility modulus errors. Let consider the signal given by a noisy receiver to an ideal correlator

$$s_1^{\text{raw}}(t) = s_1(t) + n_1(t) \quad \text{(B-1)}$$

$$\begin{bmatrix} R^{raw}_{i_1 i_2}(0) \\ R^{raw}_{q_1 i_2}(0) \end{bmatrix} = \begin{bmatrix} \cos\left(\theta_{02} - \theta_{01} + \dfrac{\theta_{q2}}{2} - \dfrac{\theta_{q1}}{2}\right) & \sin\left(\theta_{02} - \theta_{01} + \dfrac{\theta_{q2}}{2} - \dfrac{\theta_{q1}}{2}\right) \\ -\sin\left(\theta_{02} - \theta_{01} + \dfrac{\theta_{q2}}{2} + \dfrac{\theta_{q1}}{2}\right) & \cos\left(\theta_{02} - \theta_{01} + \dfrac{\theta_{q2}}{2} + \dfrac{\theta_{q1}}{2}\right) \end{bmatrix} \begin{pmatrix} V_r \\ V_j \end{pmatrix} \tag{A-14}$$

$$\begin{bmatrix} R^{raw}_{q_1 q_2}(0) \\ R^{raw}_{i_1 q_2}(0) \end{bmatrix} = \begin{bmatrix} \cos\left(\theta_{02} - \theta_{01} - \dfrac{\theta_{q2}}{2} + \dfrac{\theta_{q1}}{2}\right) & \sin\left(\theta_{02} - \theta_{01} - \dfrac{\theta_{q2}}{2} + \dfrac{\theta_{q1}}{2}\right) \\ \sin\left(\theta_{02} - \theta_{01} - \dfrac{\theta_{q2}}{2} - \dfrac{\theta_{q1}}{2}\right) & -\cos\left(\theta_{02} - \theta_{01} - \dfrac{\theta_{q2}}{2} - \dfrac{\theta_{q1}}{2}\right) \end{bmatrix} \begin{pmatrix} V_r \\ V_j \end{pmatrix} \tag{A-16}$$

$$\langle s_1^2(t) \rangle = kT_A B$$
$$\langle n_1^2(t) \rangle = kT_{R1} B. \tag{B-2}$$

Now, if we compute the measured visibility, we can write [5]

$$\mu_{12}^{raw} = \frac{\langle s_1^{raw} s_2^{raw} \rangle}{\sqrt{\langle s_1^{raw} s_1^{raw} \rangle \langle s_2^{raw} s_2^{raw} \rangle}}$$

$$= \mu_{12} \left(1 + \frac{T_{R1}}{T_{A1}}\right)^{-(1/2)} \left(1 + \frac{T_{R2}}{T_{A2}}\right)^{-(1/2)}$$

$$\mu_{12}^{raw} = g_1 g_2 \mu_{12}. \tag{B-3}$$

Now, we can compute the calibration factors out of the receiver "m" noise temperature estimation as

$$\hat{g}_m = \left(1 + \frac{\hat{T}_{Rm}}{T_A}\right)^{-(1/2)} \tag{B-4}$$

where we assumed $T_{A1} \approx T_{A2}$, and writing the receiver noise temperature as

$$T_{Rm} = \hat{T}_{Rm} + \Delta T_{Rm}. \tag{B-5}$$

We have the following expression for the calibrated visibility sample

$$\hat{\mu}_{12} = \hat{g}_1^{-1} \hat{g}_2^{-1} \mu_{12}^{raw}$$
$$= \frac{g_1 g_2}{\hat{g}_1 \hat{g}_2} \mu_{12}$$
$$= \mu_{12}(1 + \Delta\mu) \tag{B-6}$$

where $\Delta\mu$ is the amplitude error, given by

$$\Delta\mu = \frac{g_1 g_2}{\hat{g}_1 \hat{g}_2} - 1$$

$$= \left[\frac{\left(1 + \dfrac{\hat{T}_{R1}}{T_A}\right)\left(1 + \dfrac{\hat{T}_{R2}}{T_A}\right)}{\left(1 + \dfrac{\hat{T}_{R1} + \Delta T_{R1}}{T_A}\right)\left(1 + \dfrac{\hat{T}_{R2} + \Delta T_{R2}}{T_A}\right)} \right]^{1/2} - 1. \tag{B-7}$$

If we consider that $\Delta T_R \ll T_R + T_A$ and $T_{R1} \approx T_{R2}$ then, the above expression simplifies to

$$\Delta\mu = \left(1 + \frac{\Delta T_{R1}}{\hat{T}_{R1} + T_A}\right)^{-(1/2)} \left(1 + \frac{\Delta T_{R2}}{\hat{T}_{R2} + T_A}\right)^{-(1/2)} - 1$$

$$\cong \frac{1}{2} \frac{\Delta T_{R1} + \Delta T_{R2}}{\hat{T}_R + T_A}. \tag{B-8}$$

Therefore, the receiver noise temperature estimation error, gives a modulus error given by

$$\sigma_{\Delta\mu} = \frac{1}{\sqrt{2}} \frac{\sigma_{\Delta T_R}}{\hat{T}_R + T_A}. \tag{B-9}$$

Now, taking into account MIRAS receiver specifications [4] $T_R = 80$ K and $T_A = 300$ K, to reduce amplitude errors to $\sigma_{\Delta\mu} \leq 10^{-3}$ [8], receiver noise temperatures must be estimated within $\sigma_{TR} \leq 0.5$ K.

REFERENCES

[1] C. Ruf, C. Swift, A. Tanner, and D. Le Vine, "Interferometric synthesis aperture microwave radiometry for remote sensing of the earth," *IEEE Trans. Geosci. Remote Sensing* vol. 16, no. 5, Sept. 1988.
[2] A. Tanner and C. Swift, "Calibration of a synthetic aperture radiometer," *IEEE Trans. Geosci. Remote Sensing* vol. 31, no. 1, Jan. 1993.
[3] SMOS, Soil Moisture and Ocean Salinity Measurements and Radiometer Techniques Consultative Meeting, ESA.ESTEC, Noordwijk, The Netherlands, Apr. 20–22, 1995.
[4] M. Martin-Neira, Y. Menard, J. M. Goutoule, and U. Kraft, "MIRAS, A two-dimensional aperture synthesis radiometer," in *IGARSS'94*, Pasadena, CA, 1994.
[5] B. Laursen and N. Skou, "A spaceborne synthetic aperture radiometer simulated by the TUD demonstration model," in *IGARSS'94*, Pasadena, CA, 1994.
[6] A. Thompson, J. Moran, and G. Swenson, *Interferometry and Synthesis in Radio Astronomy*. New York: Wiley, 1986.
[7] J. Hagen and D. Farley, "Digital correlation techniques in radio science," *Radio Sci.*, vol. 8, pp. 775–784, 1973.
[8] J. Bará, A. Camps, I. Corbella, and F. Torres, "Bi-dimensional discrete formulation for aperture synthesis radiometer," ESA-ESTEC N. 977/92/NL/PB UPC Final Rep., Jan. 1996.

F. Torres, photograph and biography not available at the time of publication.

A. Camps, photograph and biography not available at the time of publication.

J. Bará, photograph and biography not available at the time of publication.

I. Corbella, photograph and biography not available at the time of publication.

R. Ferrero, photograph and biography not available at the time of publication.